Applied Mathematical Modelling 94 (2021) 619–634

Contents lists available at ScienceDirect

Applied Mathematical Modelling

journal homepage: www.elsevier.com/locate/apm

Non-smooth models and simulation studies of the suspension system dynamics basing on piecewise linear luz(…) and tar(…) projections

Dariusz Żardecki, Andrzej Dębowski*

Faculty of Mechanical Engineering, Military University of Technology (WAT), gen. Sylwestra Kaliskiego 2 St., 00-908 Warsaw, Poland

ARTICLE INFO

Article history:
Received 19 May 2020
Revised 7 December 2020
Accepted 24 January 2021
Available online 2 February 2021

Keywords:
Non-smooth nonlinearities
Piecewise-linear projections
Suspension system model
Simulation

ABSTRACT

Strongly nonlinear phenomena are attributes of suspension system dynamics of vehicles operated at high dynamic loads and high speeds. The causes of these phenomena are backlasches and dry friction in the mechanisms, detachments of the wheel from the roadway, impacts on the bumper elements, etc. It is well known that modelling of strong nonlinear phenomena can be based on a piecewise linear approach. To simplify the mathematical description of such phenomena, Żardecki developed special luz(…) and tar(…) projections. These piecewise-linear projections have a surprisingly simple mathematical apparatus that enables analytical operations (eg. reductions) for differential and algebraic equations and inclusions with non-smooth nonlinearities, and simplifies numerical simulations. The application of this method to model and simulation studies of the dynamics of the car steering system (including freeplay and stick-slip processes) have been reported in several authorial articles. This article presents examples related to suspension system dynamics.

1. Introduction

1.1. Vehicle suspension system models

Non-smooth nonlinearities apply to mathematical models of strongly nonlinear processes caused by abruptly changing structures and characteristics of the objects. In mechanical systems this is primarily due to the occurrence of backlash, dry friction with stiction, and collisions [1]. Numerous examples show that such processes can be characterized by strange behaviors (e.g. bifurcations, chaos) [2]. A rapid change in the mechanical structure and characteristics of the object may be the reason for non-linear vibrations, motion instability, etc., which is also observed in road vehicles [3].

In the case of modeling the "vertical dynamics" of the car, the non-smooth nonlinearities result generally from dry friction and clearance in the suspension mechanisms, functioning active elements according to the sky-hook principle, detachment of the wheel from the roadway, impact on the bumper element, etc. Strongly nonlinear processes can manifest themselves both in the case of small interactions (e.g. in stick-slip processes) and large ones (e.g. in the operation of the stopper). Such processes can be watched especially in suspension systems of the vehicles operated on uneven roads, espe-

* Corresponding author.
E-mail address: dariusz.zardecki@wat.edu.pl (D. Żardecki).

https://doi.org/10.1016/j.apm.2021.01.039
0307-904X/

cially at high speeds. In these cases the vehicle suspension elements work in extreme dynamic loads with detachments of the wheel from the roadway and with impacts on the bumper.

Meanwhile, the analysis of numerous publications on the vertical dynamics of vehicles, in particular "state-of-the-art" papers, eg. [4,5], indicate that non-smooth nonlinearities in mathematical models of suspension system dynamics are considered quite rarely. Such models appear rather only in detail studies of suspension mechanisms treated as 3D or 2D Multi Body Systems (MBS) due to their kinematic properties. Publication analyzes show that the so-called “quarter car” suspension model (1D model describing vibrations in an independent single-wheel suspension system modeled as a dual-mass system) provides the basis for researchers and engineers in describing the vehicle vertical dynamics (see review article [6]). This model in the simplest linear version is very useful not only for the presentation of the most important suspension dynamic properties, but also for the analysis or design of controllers for semi-active and active suspension systems, for analysis or design of test stands and test methods, etc. A linear “quarter car” suspension system model is used in simulation studies, as well as in analytical investigations (using Laplace / Fourier transfer functions) in time and frequency domain. Of course, it is worth undertaking research on “quarter car” suspension models, taking into account non-smooth nonlinearities. Examples of such approach are quite sporadic, eg. [7]. This article is focused on research methods regarding strongly non-linear dynamics of suspension systems, but especially with using piecewise-linear models, and special mathematical apparatus.

1.2. Piecewise-linear approach

Modelling and simulation of processes with non-smooth nonlinearities are generally quite difficult problems. In many cases, they must be modelled by differential inclusions or equations with variable structure and algebraic constraints. These models are very complicated (implicit functions, iterations), and therefore simulation calculations expand significantly over time, even if special methods, such as the method of Linear Complementary Problems (LCP) are used [8,9]. On-line simulation remains a huge challenge, as it requires fairly simple dynamic models. Piecewise-linear models seem to be an attractive proposition for many mathematical descriptions of strongly nonlinear processes. This approach takes into account the most important non-linear process features, expressed by models having switchable structures with linear segments inside.

General theory of piecewise linear systems refers to modeling, static and dynamic analysis, numerical procedures, and so on. This mathematical theory is worked up together with the non-linear theories of different dynamic objects and processes, and in the beginning - especially with the theory of electrical circuits, eg. [10,11]). So called Chua’s circuits [12] (special resistor-inductor-capacitor-diode systems) became basic electronic analog devices for studies bifurcation and chaos phenomena in piecewise-linear systems. The Chua’s circuits have their mechanical equivalents [13,14]. The theory of piecewise linear systems is developed also by the way of scientific works concerning multibody systems with freeplay (backlash with elastic compliance) and/or friction (viscous plus dry friction with stiction) in joints. Of course, piecewise linearity of models occurs frequently as a result of characteristics approximation, but also because of strong non-linear constrains [15,16]. Examples of such mechanical system models have been discussed in numerous papers (see eg. state-of-art papers [17,18]). An importance of piecewise linear systems’ theory improves because of intensive investigations of real-time control and optimization algorithms which require simplified models of systems [19–23].

There are two main approaches for piecewise linearity description [23]. The first approach is, when a model is described piece-by-piece by linear equations. The ranges of given linear variability are conditioned by constrains relations, so they are described with logical operators. In simple cases, the piecewise linearity of the model appears in its broken-line type characteristics. The second approach is, where a model is given in a compact analytic form (so called canonical form) for the full range of variations with formulas basing on linear and strong non-linear projections (type of “module” and “sign”). Here, piecewise-linear relationships are replaced by analytic formulas without logic operators.

The first approach is more general, but it leads to long-drawn-out model’s description. Even if there are special methods simplifying basic mathematical operations accomplished on multi-point piecewise-linear characteristics [24], most often such models are extreme difficult to transformation and reduction. Using the second manner of modeling those inconveniences can be avoided. Analytic description of a piecewise linear formula gives a chance for its simplification especially when a peculiar mathematic apparatus has been prepared before. Canonical forms of the piecewise linear model can be also very helpful for synthesis smart simulation procedures [25]. Of course, in many cases, calculation of compact analytic form of the model can be difficult and even impossible. In such situations we should look for mixed forms of the piecewise linear model.

Analytic description of the piecewise linear mapping uses functions and pseudo-functions which act so called basic projections. They can be created by elementary (simplest) projections, eg.

$$y = x,\ y = sgn(x) = \begin{cases} -1\ if\ x < 0 \\ 0\ if\ x = 0 \\ 1\ if\ x > 0 \end{cases},\ y = \sigma(x) = \begin{cases} 0\ if\ x \neq 0 \\ 1\ if\ x = 0 \end{cases},$$

or by their compounds and combinations, eg.

$$y = |x| = x \cdot sgn(x) = \begin{cases} -x\ if\ x \leq 0 \\ x\ if\ x \geq 0 \end{cases},\ y = sgh(x) = sgn(x) + s^* \cdot \sigma(x) = \begin{cases} -1\ if\ x < 0 \\ s^* \in [-1,\ 1]\ if\ x = 0 \\ 1\ if\ x > 0 \end{cases}$$

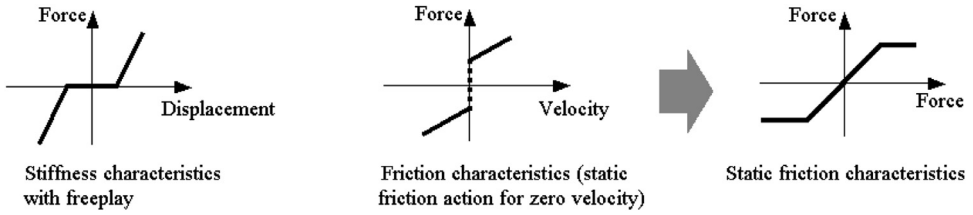

Fig 1. Typical piecewise linear characteristics for freeplay and friction expression.

Next, more complicate piecewise linear projections can be created on the base of above presented projections using simple mathematical operations as change of variable's signs, invertibility, arguments' shift, linear combinations and compounds. These new projections can be treated also as the basic ones for specific applications. Eg. the simplest piecewise linear characteristics of the diode (especially important for electronic system models) can be described as following:

$$y = diod(x) = \frac{x + |x|}{2} = x \cdot \left(\frac{1 + sgn(x)}{2}\right) = \begin{cases} 0 \ for \ x < 0 \\ x \ for \ x \geq 0 \end{cases}$$

In case of modeling discrete mechanical systems with freeplay and friction creation of the base piecewise linear projections is surprisingly simple. Though, the gist of freeplay in elementary compliance system can be expressed by the piecewise linear stiffness characteristics with "dead zone", as the friction action in elementary dissipative system – by the piecewise linear Coulomb's characteristics of kinetic friction supplemented by a piecewise linear description (saturation dependence) of static friction action and stiction effects (Fig. 1). The basic characteristics which occur in the freeplay and friction description are topologically strongly related and have analytical forms (!). This remark was a background for the idea of the luz(..) and tar(…) projections as the basic ones for freeplay and friction problems.

The luz(..) and tar(…) projections have been proposed and developed by Żardecki within a simple but very efficient mathematical apparatus (details in [26,27,28,29]). They greatly facilitate analytical transformations, especially parametrically-made formal reduction of the piecewise-linear models [30]. This is very important, because as is known from mathematical theory of dynamic systems' sensitivity, ensuring a proper continuity of a reduced model requires some regularity of transformations that can be obtained when they are implemented in a parametric way (Hadamard postulate).

The luz(…) and tar(…) projections and their mathematical apparatus have been used with success in many applications, especially concerning the friction theory (stick slip processes, static friction indeterminacy problems) [31,32] and vehicle steering systems dynamics (where problems of a gear freeplay and kin-pin dry friction are evident) [33,34,35,36].

This paper is extended version of the paper presented on 15th DSTA Conference [37]. It contains (p.2) short information on the luz(…) and tar(…) projections and their mathematical apparatus, and then (p.3, p.4, p.5) describes the method of application these projections to study suspension system models and vehicle vertical dynamics.

2. Piecewise linear luz(…) and tar(…) projections

The piecewise linear luz(…) and tar(…) projections are defined as following:

$$luz(x, a) = x + \frac{|x - a| - |x + a|}{2}, \tag{1}$$

$$tar(x, a) = x + a \cdot s^* \tag{2}$$

where $s^* \in [-1, 1]$, $a \geq 0$

Note, that these projections are like inverse functions (see Fig. 2), which means that:

$$luz(x, a) = tar^{-1}(x, a), \tag{3}$$

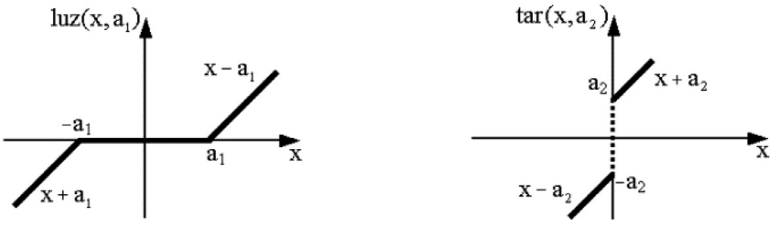

Fig. 2. Topological interpretation of luz(…) and tar(…) projections.

$$tar(x,a) = luz^{-1}(x,a) \tag{4}$$

The luz(...) and tar(...) projections have surprisingly simple properties. Their formulas compose some mathematical apparatus. Here only example formulas are shown. Constants a, k,... appearing in the formulas are non-negative.

$$luz(-x,a) = -luz(x,a), \tag{5}$$

$$tar(-x,a) = -tar(x,a) \tag{6}$$

$$luz(luz(x,a),b) = luz(x,a+b), \tag{7}$$

$$tar(tar(x,a),b) = tar(x,a+b) \tag{8}$$

$$k \cdot luz(x,a) = luz(k \cdot x, k \cdot a), \tag{9}$$

$$k \cdot tar(x,a) = tar(k \cdot x, k \cdot a) \tag{10}$$

$$k_1 \cdot tar(x,a_1) + k_2 \cdot tar(x,\ a_2) = (k_1+k_2) \cdot \left(x, \frac{k_1 \cdot a_1 + k_2 \cdot a_2}{k_1+k_2}\right) \tag{11}$$

If $luz(y,\ b) = k{\cdot}luz(x - y,\ a)$ then

$$luz(y,b) = \frac{k}{k+1} \cdot luz(x,a+b) \tag{12}$$

Note: For a linear system ($a = b = 0$) it means the well known dependence $y = \frac{k}{k+1} \cdot x$
If

$$\varepsilon \cdot \dot{x}(t) \in y(t) - b \cdot tar(x(t),\ a) \text{ and } \varepsilon \to 0 \text{ then } x(t) = luz\left(\frac{y(t)}{b}, a\right) \tag{13}$$

Extensive lists of mathematical theorems (also with proofs) are described in the Żardecki's papers.

The luz(…) and tar(…) projections can be used as basic projections for description different piecewise linear characteristics (Fig. 3). Such descriptions depends on researcher's inventions a lot. More complicate dependences can be expressed also by projections' series.

These examples concern characteristics with symmetry in relation to the point (0,0). When the symmetry deals with the shifted point the well-known rules of description of function with deflexed arguments should be applied. When characteristics has not any symmetries it can be treated as a part of full symmetrical characteristics having large deflection parameter (Fig. 4).

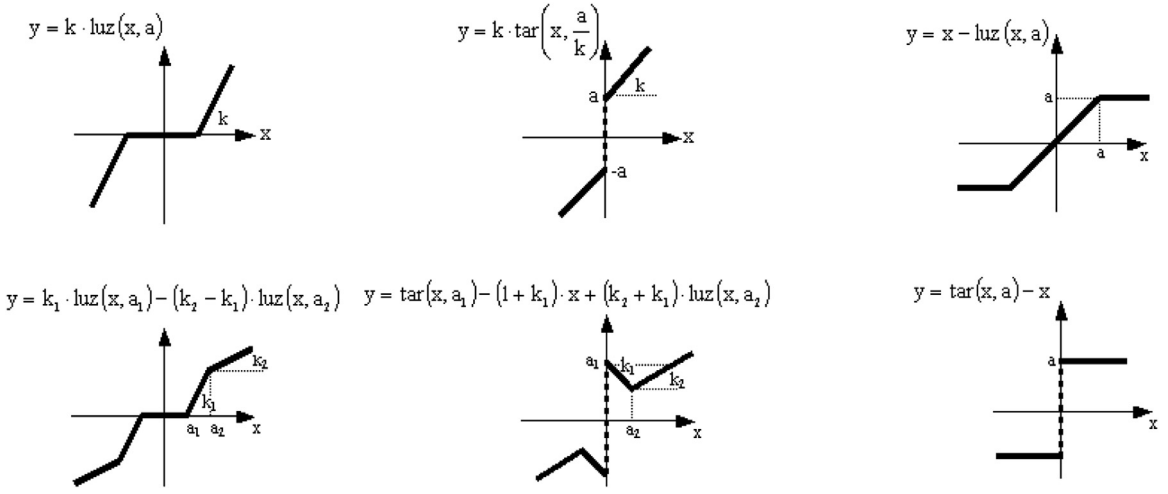

Fig. 3. Examples of piecewise linear characteristics basing on luz(…) or/and tar(…).

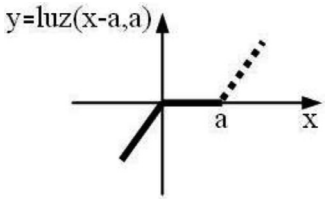

Fig. 4. Example of piecewise linear asymmetric characteristics. Here a>>0.

3. Modeling of MBS-type suspension subsystem

The luz(...) and tar(...) mathematical apparatus is very useful in formal synthesis MBS-type non-smooth systems. Representative example expressing the method of modeling corresponds with models of suspension system having clearances and limiters of the movements.

This system (Fig. 5) is a combination of four solid elements through elastic elements. There is a clearance between elements 2 and 3. Solid elements 2 and 3 have very low masses. The stiffness between elements 2 and 3 is very high. We will assume that dynamic excitations are small enough to justify not including plastic collisions in the physical model.

Notation and assumptions:

z_1, z_2, z_3, z_4 – placements of solid elements,

F_1, F_2, F_3, F_4 – external forces; we will assume that $F_2 = 0$, $F_3 = 0$,

t – time,

M_1, M_2, M_3, M_4 – masses, $M_1, M_4 \gg M_2, M_3$; we will assume that $M_2 = 0$, $M_3 = 0$,

K_{12}, K_{23}, K_{34} – stiffness coefficients, $K_{23} \gg K_{12}, K_{34}$; we will assume that $K_{23} \to \infty$,

$(z_3 - z_4)_0$ – clearance parameter.

Using Lagrange second type equations of motion one obtains initial form of the model:

$$M_1 \cdot \ddot{z}_1(t) + K_{12} \cdot (z_1(t) - z_2(t)) = F_1(t), \tag{14}$$

$$M_2 \cdot \ddot{z}_2(t) - K_{12} \cdot (z_1(t) - z_2(t)) + K_{23} \cdot luz((z_2(t) - z_3(t)),\ (z_2 - z_3)_0) = 0, \tag{15}$$

$$M_3 \cdot \ddot{z}_3(t) - K_{23} \cdot luz((z_2(t) - z_3(t)),\ (z_2 - z_3)_0) + K_{34} \cdot (z_3(t) - z_4(t)) = 0, \tag{16}$$

$$M_4 \cdot \ddot{z}_4(t) - K_{34} \cdot (z_3(t) - z_4(t)) = F_4(t). \tag{17}$$

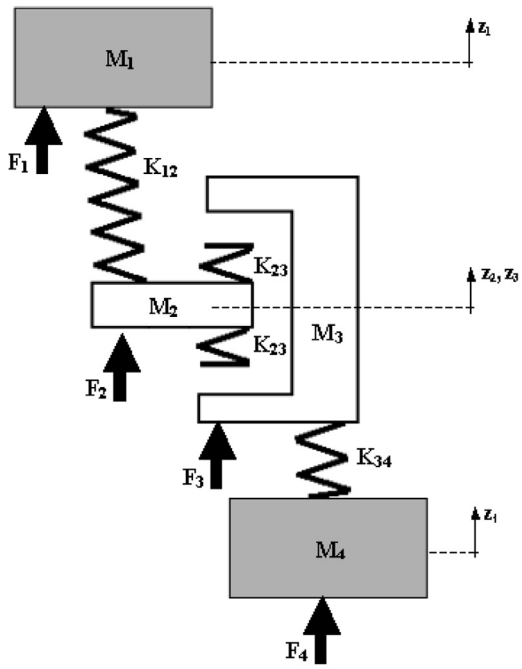

Fig. 5. Substitute mechanical scheme of MBS-type suspension subsystem.

When $M_2 = 0, M_3 = 0$ the model is reduced to the differential - algebraic form. Algebraic non-linear constraints equations are:

$$-K_{12} \cdot (z_1(t) - z_2(t)) + K_{23} \cdot luz((z_2(t) - z_3(t)), (z_2 - z_3)_0) = 0, \tag{18}$$

$$-K_{23} \cdot luz((z_2(t) - z_3(t)), (z_2 - z_3)_0) + K_{34} \cdot (z_3(t) - z_4(t)) = 0. \tag{19}$$

Release from these equations and elimination of z_2, z_3 will be here made using basic formulas of luz(...) and tar(...) mathematical apparatus. These mathematical operations are following:

- Firstly, in order to reduce, we determine $z_3(t)$ from the first equation of constraints (18):

$$z_3(t) = z_2(t) - tar\left(\left(\frac{K_{12}}{K_{23}}(z_1(t) - z_2(t))\right), (z_2 - z_3)_0\right) \tag{20}$$

- Then, after setting to the second Eq. (19), we have

$$K_{34} \cdot \left(z_2(t) - tar\left(\left(\frac{K_{12}}{K_{23}}(z_1(t) - z_2(t))\right), (z_2 - z_3)_0\right) - z_4(t)\right) = K_{12} \cdot (z_1(t) - z_2(t)) \tag{21}$$

Hence we obtain successively:

$$z_2(t) - z_4(t) = \frac{K_{12}}{K_{34}}(z_1(t) - z_2(t)) + tar\left(\left(\frac{K_{12}}{K_{23}}(z_1(t) - z_2(t))\right), (z_1 - z_2)_0\right) \tag{22}$$

$$z_2(t) - z_4(t) = \frac{K_{12}}{K_{34}}(z_1(t) - z_2(t)) + \frac{K_{12}}{K_{23}} tar\left((z_1(t) - z_2(t)), \left(\frac{(z_2 - z_3)_0}{\frac{K_{12}}{K_{23}}}\right)\right) \tag{23}$$

$$z_2(t) - z_4(t) = \frac{K_{12}}{K_{34}} tar((z_1(t) - z_2(t)), 0) + \frac{K_{12}}{K_{23}} tar\left((z_1(t) - z_2(t)), \left(\frac{(z_2 - z_3)_0}{\frac{K_{12}}{K_{23}}}\right)\right) \tag{24}$$

- Using the formula (11) we have:

$$z_2(t) - z_4(t) = \left(\frac{K_{12}}{K_{34}} + \frac{K_{12}}{K_{23}}\right) tar\left((z_1(t) - z_2(t)), \left(\frac{(z_2 - z_3)_0}{\frac{K_{12}}{K_{34}} + \frac{K_{12}}{K_{23}}}\right)\right) \tag{25}$$

And then

$$z_1(t) - z_2(t) = \frac{1}{\frac{K_{12}}{K_{34}} + \frac{K_{12}}{K_{23}}} luz((z_2(t) - z_4(t)),\ (z_2 - z_3)_0) \tag{26}$$

$$z_1(t) - z_2(t) = \frac{1}{\frac{K_{12}}{K_{34}} + \frac{K_{12}}{K_{23}}} luz(((z_1(t) - z_4(t)) - (z_1(t) - z_2(t))),\ (z_2 - z_3)_0) \tag{27}$$

i.e.

$$luz((z_1(t) - z_2(t)), 0) = \frac{1}{\frac{K_{12}}{K_{34}} + \frac{K_{12}}{K_{23}}} luz(((z_1(t) - z_4(t)) - (z_1(t) - z_2(t))),\ (z_2 - z_3)_0) \tag{28}$$

Using formulas (12) we obtain a disentanglement form

$$z_1(t) - z_2(t) = \frac{\frac{1}{\frac{K_{12}}{K_{34}} + \frac{K_{12}}{K_{23}}}}{\frac{1}{\frac{K_{12}}{K_{34}} + \frac{K_{12}}{K_{23}}} + 1} luz((z_1(t) - z_4(t)),\ (z_2 - z_3)_0\ ) \tag{29}$$

By combination of the constraints Eqs. (18), (19) we receive

$$z_1(t) - z_2(t) = \frac{K_{34}}{K_{12}} \cdot (z_3(t) - z_4(t)) \tag{30}$$

Then

$$z_3(t) - z_4(t) = \frac{K_{12}}{K_{34}} \frac{\frac{1}{\frac{K_{12}}{K_{34}} + \frac{K_{12}}{K_{23}}}}{\frac{1}{\frac{K_{12}}{K_{34}} + \frac{K_{12}}{K_{23}}} + 1} luz((z_1(t) - z_4(t)),\ (z_2 - z_3)_0\ ) \tag{31}$$

Finally, assuming a substitute stiffness parameter

$$K_{14} = \frac{1}{\frac{1}{K_{12}} + \frac{1}{K_{23}} + \frac{1}{K_{34}}} \tag{32}$$

we obtain the model without constraints equations, and without variables $z_2(t)$ and $z_3(t)$:

$$M_1 \cdot \ddot{z}_1(t) + K_{14} \cdot luz((z_1(t) - z_4(t)),\ (z_2 - z_3)_0) = F_1(t) \tag{33}$$

$$M_4 \cdot \ddot{z}_4(t) - K_{14} \cdot luz((z_1(t) - z_4(t)),\ (z_2 - z_3)_0) = F_4(t) \tag{34}$$

This model describes the dynamics of the system in the presence of clearance and infinitely high stiffness (i.e. limiter) in meshing.

4. Modeling and simulation of quarter-car suspension system dynamics

4.1. Piecewise-linear model of quarter car suspension system dynamics

A simplified model presented in this paper concerns an independent suspension system of a passenger car driving with constant speed on a straight uneven road. The substitute mechanical scheme of the system (Fig. 6) includes the most important suspension and tire attributes related to the description of vertical movement dynamics, i.e. piecewise linear suspension elasticity (including limiter action), viscous friction (damping) and dry friction in the shock absorber, as well as piecewise linear elasticity in the tire – road interactions, taking into account wheel detachment from the road surface. More detailed description of tire motion is not analyzed. As the presented non-linear model was supposed to be a development of the standard linear single-wheel suspension models, a very simplified point description of the cooperation between the wheel and the road (but with the wheel detachment effect) was used in it. A detailed description of the wheel-road interaction (going beyond framework of this article), also based on the projections luz(...) and tar(...) is prepared. It takes into account the 3-dimensional description, the stick-slip phenomenon, and the phenomenon of relaxation. This model is unfortunately very extensive. A publication on the description of the wheel-road interaction is planned after stand and simulation experiments.

Characteristics $F_{S21}(z_2 - z_1)$, $F_{S10}(z_1 - z_0)$ express spring properties of the suspension system and tire, while $F_{D21}(\dot{z}_2 - \dot{z}_1)$ – friction (dry plus viscous) properties. Piecewise linear description of these force characteristics presented in Fig. 1 can be described using luz(...) and tar(...) projections, as follows:

$$F_{S21}(z_2 - z_1) = K_{21}(z_2 - z_1) + (K_{21L} - K_{21})luz((z_2 - z_1),\ \Delta z_{21L}) \tag{35}$$

$$F_{S10}(z_1 - z_0) = K_{10}luz(z_1 - z_0 - a, a)\ a \gg 0 \tag{36}$$

Note: Wheel detachment from the road surface means that in such state the force should be equal zero. This is described by specific characteristics type of $k{\cdot}luz(x - a, a)$, where shift parameter a has a “big” value due to x.

$$F_{D21}(\dot{z}_1 - \dot{z}_2) = C_{21}tar\left((\dot{z}_1 - \dot{z}_2), \frac{F_{D210}}{C_{21}}\right) \tag{37}$$

Notation:
t - time
(0XZ) - global coordinate system

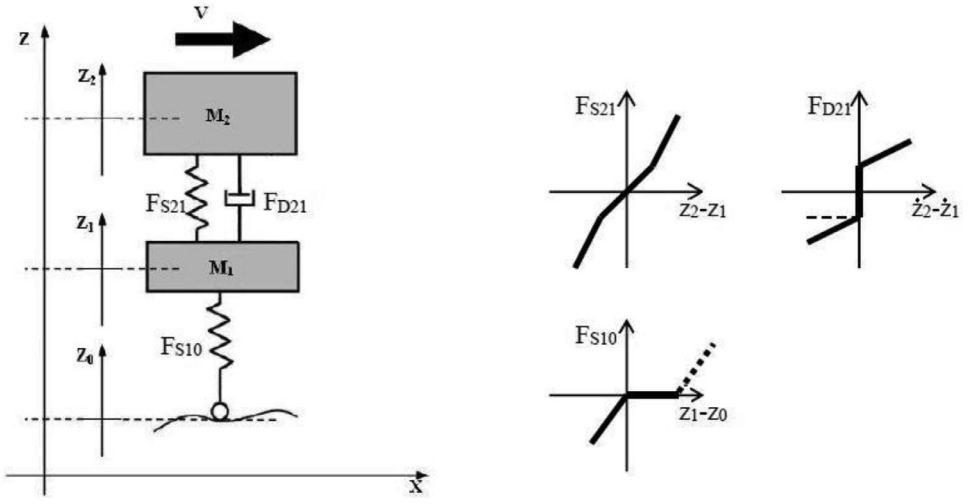

Fig. 6. Substitute mechanical scheme of suspension system with piecewise liner spring and dissipative force characteristics.

$z_0(t)$ - road profile as a function of time
$z_1(t)$ - vertical displacement of the wheel centre
$z_2(t)$ - vertical displacement of the sprung mass
Δz_{21L} - maximum deformation of the suspension system without limiter's action
K_{10} - stiffness coefficient of the tire
K_{21} - stiffness coefficient of the suspension
K_{21L} - stiffness coefficient of the suspension with limiter's action
C_{21} - damping coefficient of the shock absorber
F_{D210} - maximum dry friction (we assume the same values for static and kinetic dry friction)
M_1 - unsprung mass (of the wheel)
M_2 - sprung mass (of the quarter carbody).
g - gravitation acceleration.

Initial mathematical model describing motions in local coordinates is done by two differential inclusions (inclusions because of the dry friction action):

$$M_1\ddot{z}_1(t) + C_{21}tar\left((\dot{z}_1(t) - \dot{z}_2(t)), \frac{F_{D210}}{C_{21}}\right) + K_{21}(z_1(t) - z_2(t)) + (K_{21L} - K_{21})luz\ (z_1(t) - z_2(t), \Delta z_{21L}) + K_{10}luz(z_1(t) - z_0(t) - a, a) + M_1 g \in 0 \tag{38}$$

$$M_2\ddot{z}_2(t) + C_{21}tar\left((\dot{z}_2(t) - \dot{z}_1(t)), \frac{F_{D210}}{C_{21}}\right) + K_{21}(z_2(t) - z_1(t)) + (K_{21L} - K_{21})luz(z_2(t) - z_1(t), \Delta z_{21L}) + M_2 g \in 0 \tag{39}$$

Using methodology presented in [11], these differential inclusions create the model in differential equation form (here with variable structure).

$$M_1\ddot{z}_1(t) = \begin{cases} -F_{D210}sgn(\dot{z}_1(t) - \dot{z}_2(t)) + F_1(t) & if \quad \dot{z}_1(t) \neq \dot{z}_2(t) \\ \dfrac{M_1(F_1(t) + F_2(t))}{M_1 + M_2} + luz\left(\dfrac{M_2F_1(t) - M_1F_2(t)}{M_1 + M_2},\ F_{D210}\right) & if \quad \dot{z}_1(t) = \dot{z}_2(t) \end{cases} \tag{40}$$

$$M_2\ddot{z}_2(t) = \begin{cases} F_{D210}sgn(\dot{z}_1(t) - \dot{z}_2(t)) + F_2(t) & if \quad \dot{z}_1(t) \neq \dot{z}_2(t) \\ \dfrac{M_2(F_1(t) + F_2(t))}{M_1 + M_2} - luz\left(\dfrac{M_2F_1(t) - M_1F_2(t)}{M_1 + M_2},\ F_{D210}\right) & if \quad \dot{z}_1(t) = \dot{z}_2(t) \end{cases} \tag{41}$$

where:

$$F_1(t) = -C_{21}(\dot{z}_1(t) - \dot{z}_2(t)) - K_{21}(z_1(t) - z_2(t)) - (K_{21L} - K_{21})luz((z_1(t) - z_2(t)), \Delta z_{21L}) \tag{42}$$
$$- K_{10}luz\ (z_1(t) - z_0(t) - a, a) - M_1 g \tag{42}$$

$$F_2(t) = -F_1(t) + K_{10}luz(z_1(t) - z_0(t) - a, a) + M_1 g - M_2 g \tag{43}$$

Because of gravitation forces, the time series of variables $z_1(t)$ and $z_2(t)$ occur around steady states z_{10} and z_{20} that result from the action of gravity. These steady states create initial conditions for processes resulting from road unevennesses. Note, that z_{10} and z_{20} can be treated as the steady state results of action of gravitation forces modelled as the functions $M_1 \cdot g \cdot 1(t)$ and $M_2 \cdot g \cdot 1(t)$ (1(t) – Heaviside function) applied to the system model with zeros initial conditions.

The time course of the road profile is an excitation in the model. With the given profile $z_0(x)$, an appropriate transformation of the variables should be performed. When the vehicle is traveling at a constant speed V, then $z_0(x(t)) = z_0(V(t))$, which means that the parameter V is a time scaling factor. For a random, poliharmonic or sinusoidal course of variable $z_0(V(t))$, one obtains slow changing waveforms – for small speeds, and fast changing waveforms – for high speeds.

In a similar way, we can treat input signal caused by a single hummock (Fig. 7).

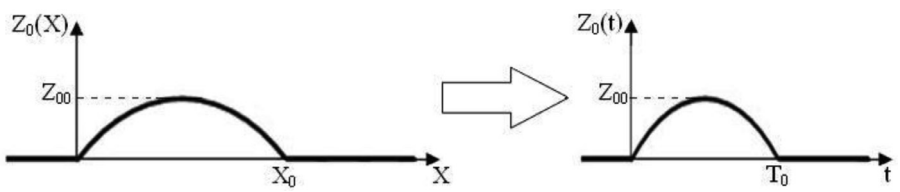

Fig. 7. Puls - type input signal $z_0(t)$.

This input signal can be described as the half period of the sinusoidal signal:

$$z_0(t) = Z_{00} \sin\left(\frac{\pi}{T_0} t\right)(1(t) - 1(t - T_0)) \tag{44}$$

where

$$T_0 = \frac{X_0}{V} \tag{45}$$

X_0 – hump length
Z_{00} – hump height
V – car sped
Note, that for typical sinusoidal signal (tare type road unevenesses simulated experimentally by test rig):

$$z_0(t) = Z_{00} \sin(2\pi f_0 t) 1(t) \tag{46}$$

where f_0 – frequency of input signal. Note that f_0 can be interpreted as

$$f_0 = 1/(2T_0) = V/(2X_0). \tag{47}$$

For detection peculiar states of the model special temporary indexes are defined:

$$q_{10}(t) = 1 + sgn(luz(z_1(t) - z_0(t) - a, a)) = \begin{cases} 1 & if \quad z_1(t) - z_0(t) \geq 0 \quad Wheel\ datachment \\ 0 & if \quad z_1(t) - z_0(t) < 0 \quad Lack\ of\ wheel\ datachment \end{cases} \tag{48}$$

$$q_{21}(t) = sgn(luz(z_1(t) - z_2(t), \Delta z_{12})) = \begin{cases} -1 & if \quad z_2(t) - z_1(t) < -\Delta z_{21} \quad Low\ limiter\ action \\ 0 & if \quad -\Delta z_{21} \leq z_2(t) - z_1(t) \leq \Delta z_{21} \quad No\ limiter\ actrion \\ 1 & if \quad z_2(t) - z_1(t) > \Delta z_{21} \quad Upper\ limiter\ action \end{cases} \tag{49}$$

4.2. Simulation of quarter-car suspension system motions

The simulation program has been worked up on the basis of the model presented in p.4.1. The program Fig. 8 was developed in the LabVIEW software system with Control Design and Simulation module, and with using numerical and graphic procedures described in authors' articles [35,36]. The problem of selecting the method and the integration step have been analyzed in great detail and was preceded by a series of numerical tests. In this case, the Runge-Kutta 4 method with step 0.001 s was used.

According to this program, simulation processes contain two phases of calculations: the first – calculation of initial conditions of variables z_{10} and z_{20}, the second – calculation of the responses $z_1(t)$, $z_2(t)$ at a given excitation $z_0(t)$. The start time of $z_0(t)$ is determined experimentally with some large reserve (note that the length of the temporary forms of output signals depends on the parameters of the suspension). The idea of these calculations is shown in Fig. 9.

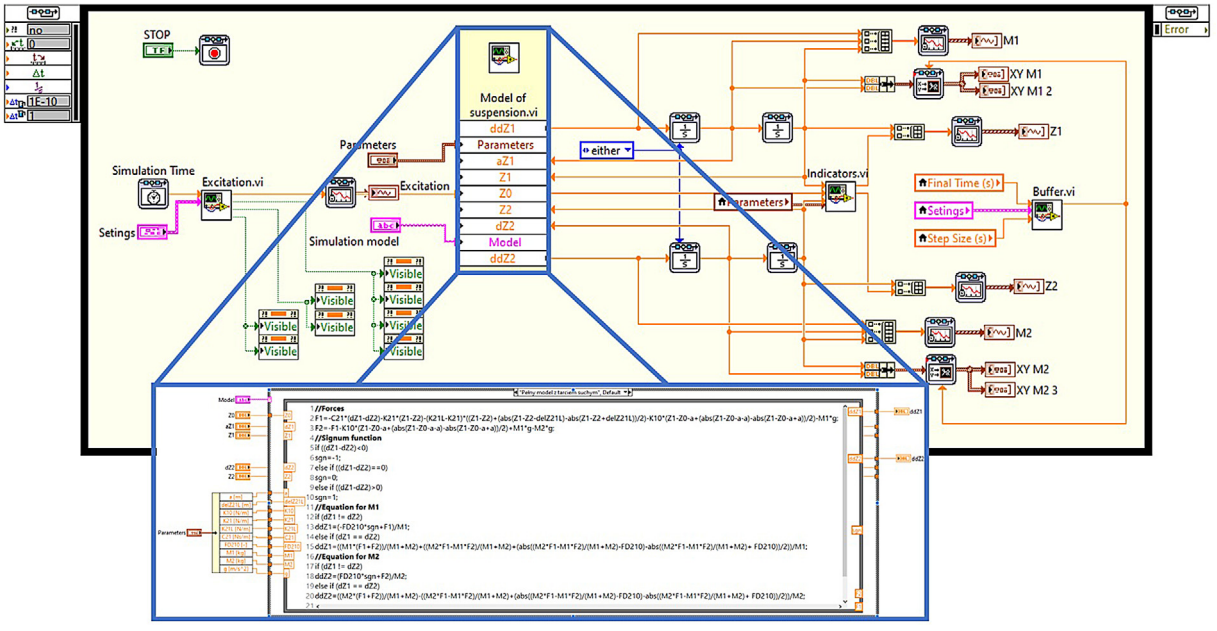

Fig. 8. Screen view with simulation program code.

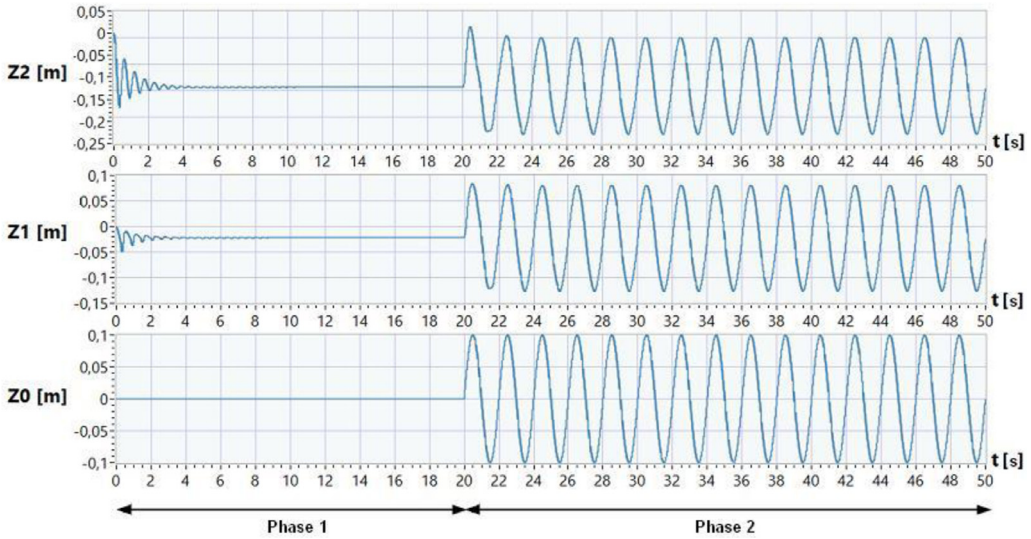

Fig. 9. Example two phase simulation process (here sinusoidal excitation begins when t = 20 s).

Table 1
List of parameters of the simulation model. Their values are in SI system.

Parameter	Value	Description
M_1	30	Unsprung mass (of the wheel)
M_2	300	Sprung mass (of the quarter car body)
C_{21}	2000	Damping coefficient of the shock absorber
F_{D210}	0.2	Maximum dry friction (the same values for static and kinetic dry friction)
K_{21}	40000	Stiffness coefficient of the suspension
K_{21L}	300000	Stiffness coefficient of the suspension with limiter's action
K_{10}	200000	Stiffness coefficient of the tire
Δz_{21L}	0.14	Maximum deformation of the suspension system without limiter's action
g	9.81	Gravitation acceleration
When pulse-type input signal		
Z_{00}	0.15	Hump height
X_0	0.5	Hump length
V	0.5; 1.0; 1.5; 2.0; 2.5; 3.0; 3.5; 4.0; 4.5; 5.0; 5.5; 6.0; 6.5; 7.0; 7.5; 8.0; 8.5; 9.0; 9.5; 10.0	Car speed
When sinusoidal input signal		
Z_{00}	0.15	Amplitude
f_0	0.5; 1.0; 1.5; 2.0; 2.5; 3.0; 3.5; 4.0; 4.5; 5.0; 5.5; 6.0; 6.5; 7.0; 7.5; 8.0; 8.5; 9.0; 9.5; 10.0	Frequency

Simulation investigations presented in this article concern of two types of input signals $z_0(t)$: pulse type signal (44), and sinusoidal signal (46). Simulation results contain not only time curses $z_1(t)$, $z_2(t)$ but also indexes $q_{10}(t)$, $q_{21}(t)$. For periodic excitations, simulation results are presented also with using phase plots $\dot{z}_{10}(z_{10})$ and $\dot{z}_{21}(z_{21})$. These phase plots contain special marker lines corresponding with non-zero values of indicator signals.

The following examples of research calculations were made on the data presented in Table 1. They concern a hypothetical passenger car, but their values do not differ much from the data of the real vehicle. To determinate of data, the earlier studies on single-wheel linear models quoted in the review paper [6] were used. Of course, the model validation may be of a qualitative nature in this case. For quantitative validation, numerical data and experimental results for a specific vehicle should be used. Such works are planned.

The results of simulations are presented in Figs. 10–13.

4.3. Discussion of simulation results

The calculation results presented in Figs. 10–13, although they relate to a selected fragment of simulation research, authorize to draw a number of interesting observations and conclusions.

At the outset, we analyze the results of the simulation with pulse excitation (Figs. 10, 11). For the smallest of the assumed speeds V = 0.5 m/s the suspension system behaved like a linear system (zeroing of both indicators $q_{10}(t)$, $q_{21}(t)$). At the next value of speed, i.e. at V = 1.0 m/s, wheel detachment is observed, as well as a short-term impact on the lower stop occurring after the cessation of the wheel detachment. The waveforms at the next V values show significant irregularities,

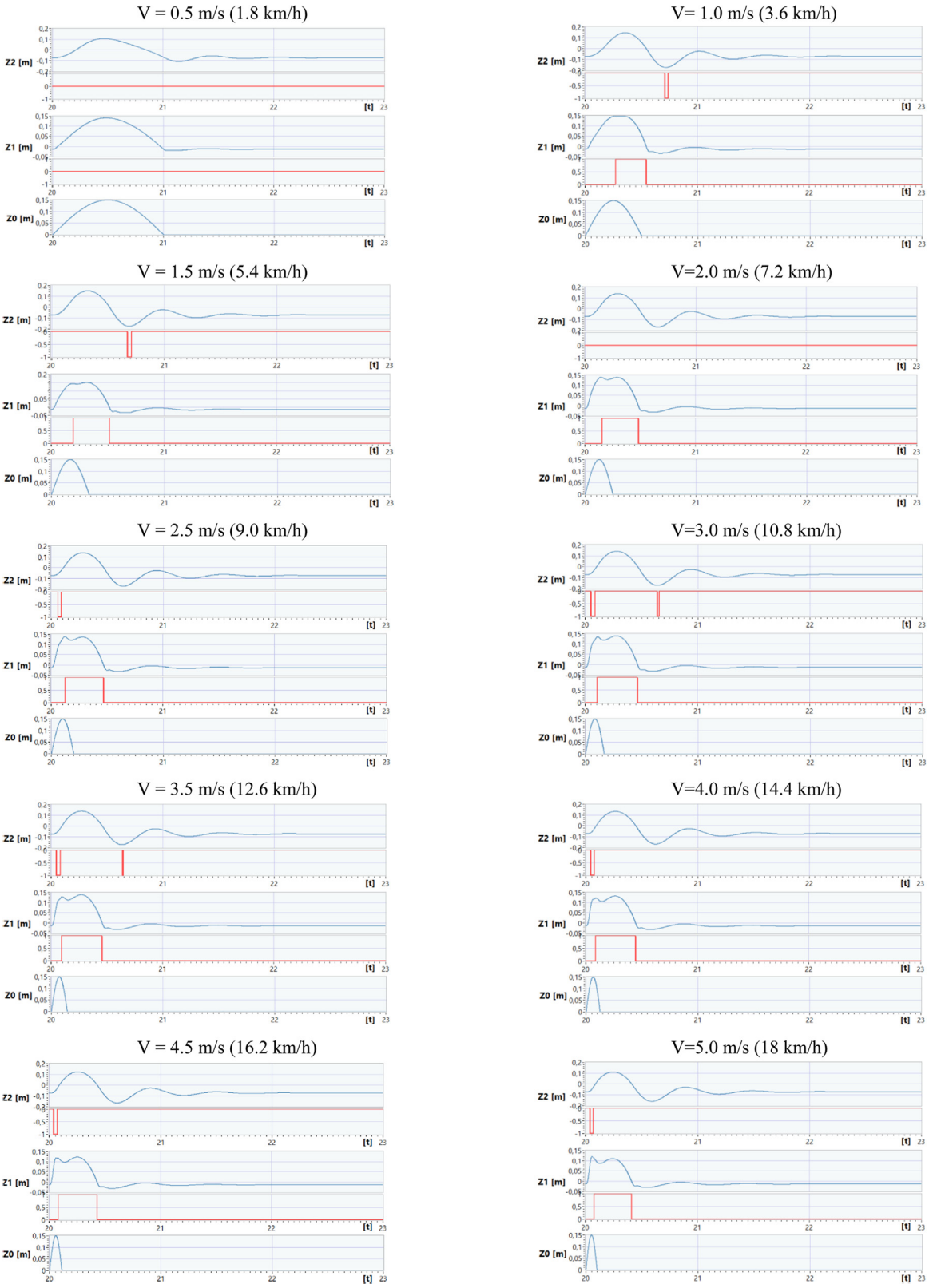

Fig. 10. Example simulation results for pulse type excitation.

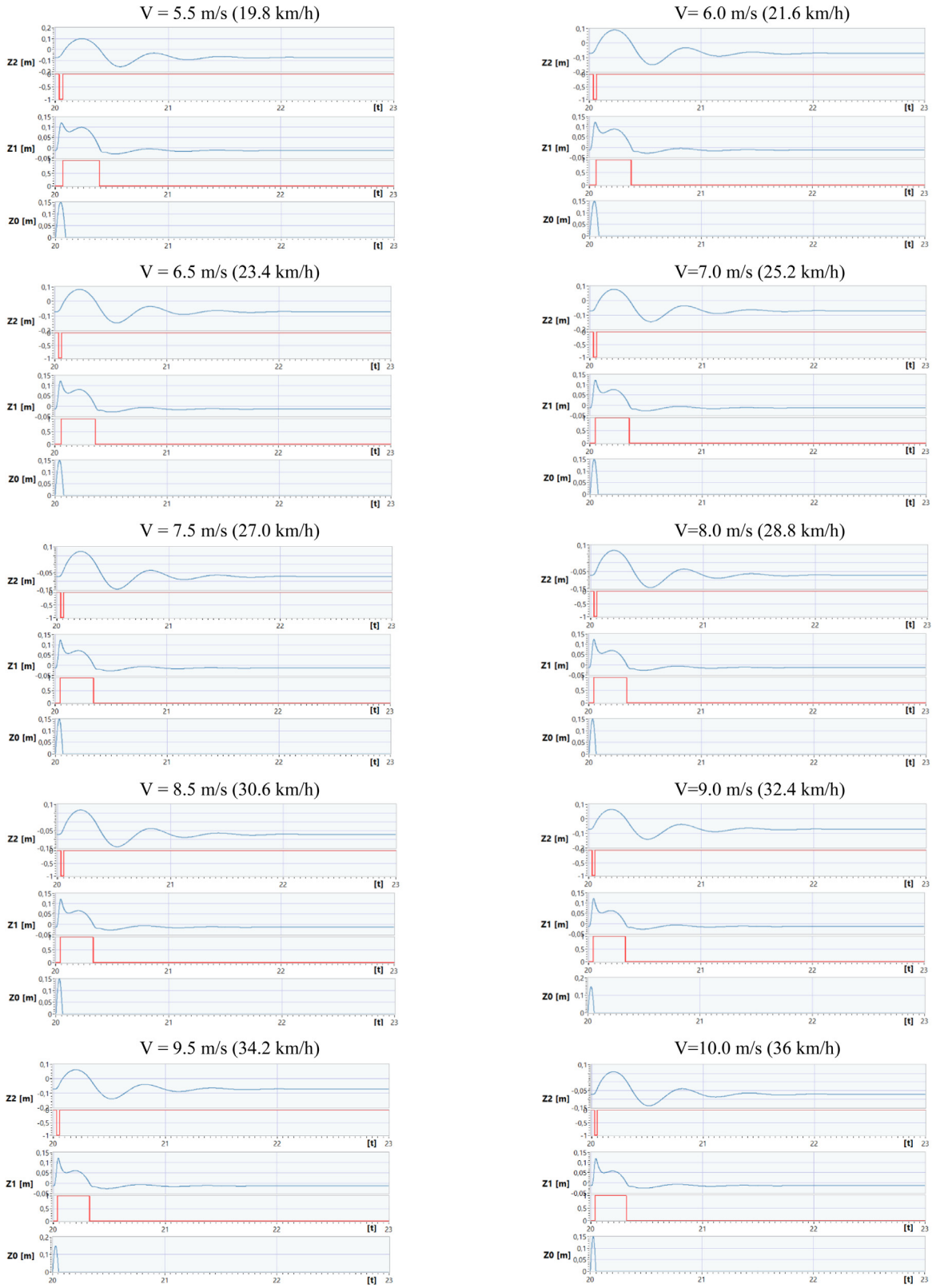

Fig. 11. Example simulation results for pulse type excitation.

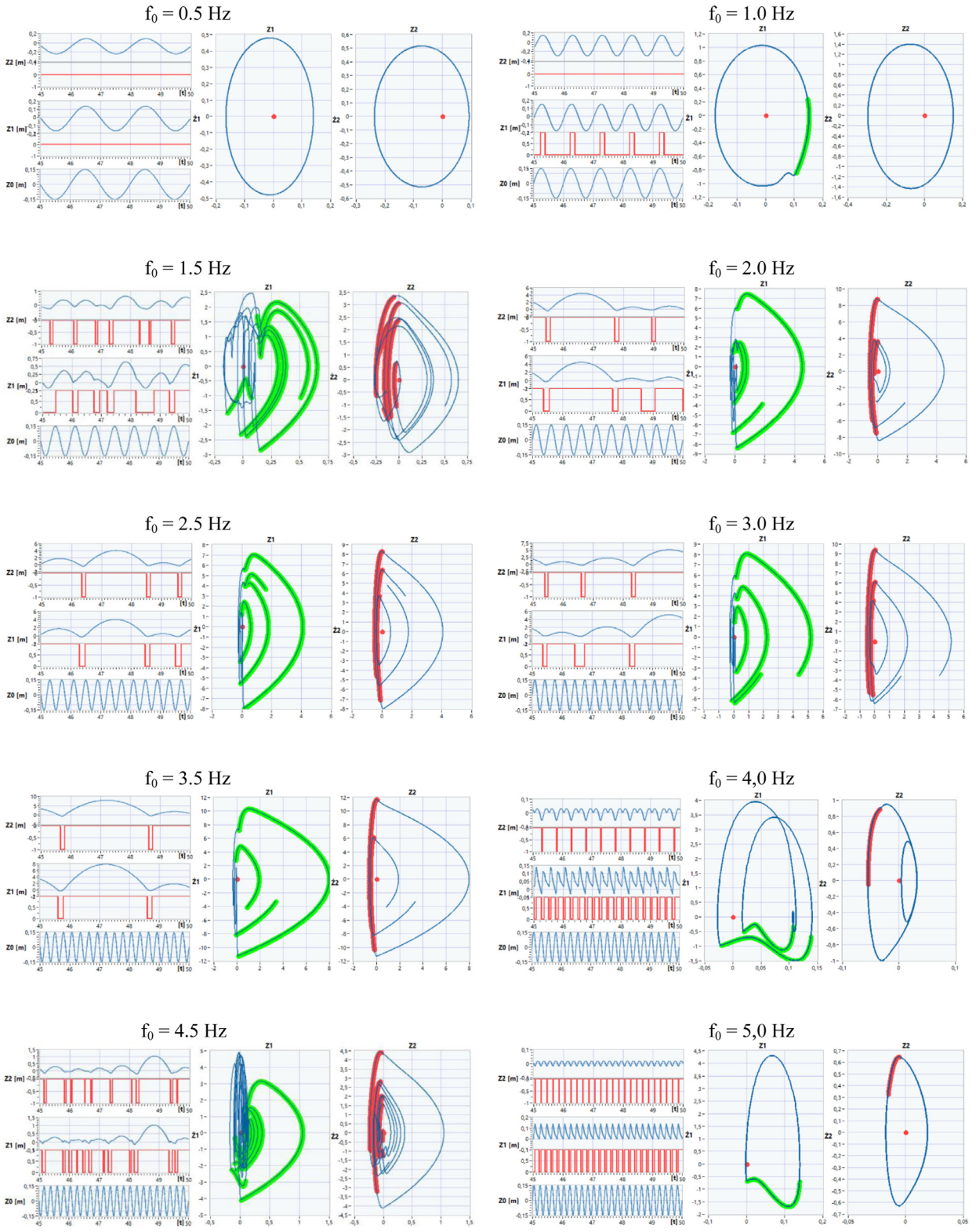

Fig. 12. Example simulation results for sinusoidal excitation.

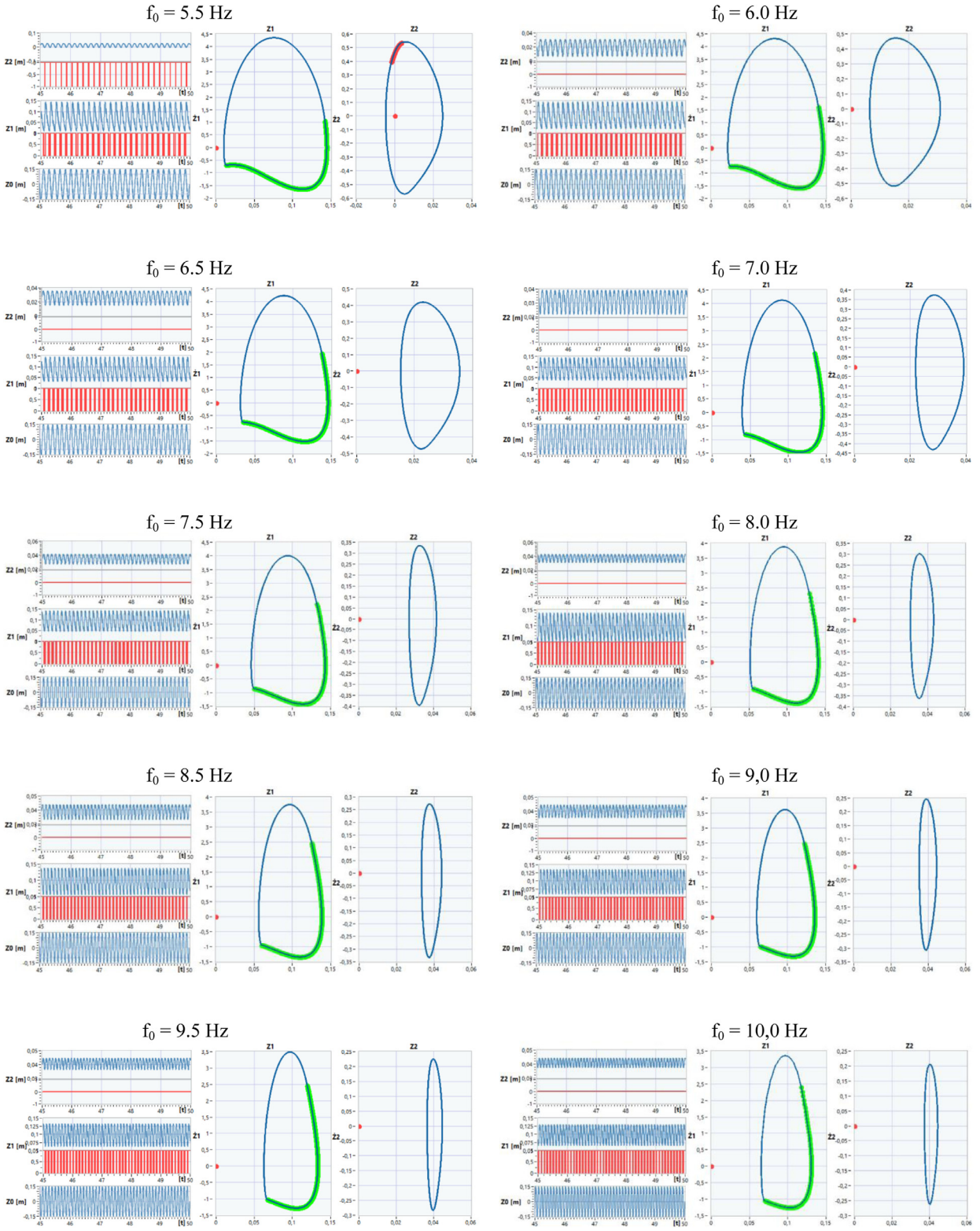

Fig. 13. Example simulation results for sinusoidal excitation.

e.g. at V = 2.0 m/s you can see the wheel detachment, but without hit the bumper, while at V = 3.0 m/s you can see the wheel detachment and double impact on the bottom stop. At speeds in the range of [5.0,10.0] m/s, the simulated waveforms behave in a regular manner - when the wheel detaches, a lower limiter impact occurs. Of course, as the speed increases, the duration of the wheel detachment slightly increases, but such an increase is more visible in the low speed range. This fact can be easily explained. We note that an important measure of the "violence" of the input signal $z_0(t)$ with the unchanged Z_{00} amplitude is the value of its duration T_0. Because the relationship $T_0(V)$ is a hyperbolic function (45), whose values decrease as V increases (for small V values relatively quickly, then slowly), so for some larger V their effect on T_0 is relatively small. This can be seen when comparing the results from Figs. 10 and 11. Significant differences can be seen only for V in the "small values" range (for vehicle speeds from several to a dozen or so km/h), in this case for $V \in [0.5, 5.0]$ m/s. Thus, the irregularity of the course of solutions has a local feature when the vehicle speed is changed.

Simulations carried out in the case of impulse interaction for subsequent velocity values V have their direct references to the simulations for the case of sinusoidal interaction implemented for the subsequent values of the frequency f_0 of the input signal. This is demonstrated by the relationship (47). Therefore, it seems reasonable to attempt to correlate the analysis of results for both types of excitations (only attempt, because as we know in the case of non-linear systems, such simple transferring of conclusions may turn out to be an error).

Now we discuss simulations for sinusoidal excitations. Of course such analysis concerns of a section of output signals after the time of cessation of transient signals resulting from the fact of inclusion of sinusoidal input signal. In these cases also the phase plots are interesting and useful. For small values of frequency $f_0 = 0.5$ Hz the output signals can be treated as signals from a linear system. (no detachments, no stop actions). Hear phase plots are typical ellipses. Non-linear effect appears for $f_0 = 1.0$ Hz. It is visible also in phase plots. For next rather small frequencies from the range [1.5, 5.0] Hz irregular (chaos - like) effects can be observed. For next higher frequencies output signals $z_1(t)$ and $z_2(t)$ have regular forms typical for periodic poliharmonic signals. Note that in these case phase plots have forms of distorted ellipses.

So, we can observe that in this piecewise-linear system there is enough powerful correlation between results obtained for impulse-type and sinusoidal excitation.

5. Conclusions

The presented method of modeling strong non-linerities in vehicle suspension system and non-linear vertical dynamics of a vehicle, the method based on piecewise linear luz(…) and tar(…) projections is very effective. It can be quite easily applied to more sophisticated models of suspension systems, also to 3D models. In this case, it is necessary to enter vector dependencies, which will result in a more complex non-linear description. This also applies to the spatial description of the tire - road interaction.

The method based on piecewise linear luz(…) and tar(…) projections is also very useful in simulation investigations. The examples of such research presented in this article show us some huge fields of very attractive studies for specialists in vehicle system dynamics, non-linear mechanics, and mathematics. Sensitivity studies (with variation of mass, stiffness and friction parameters) should provide answers to many next interesting questions.

Declaration of Competing Interest

None.

References

[1] B. Brogliatto B., Nonsmooth mechanics: Models, Dynamics and Control, Springer, 1999.
[2] J. Awrejcewicz J., C.H. Lamarque, Bifurcation and Chaos in Nonsmooth Mechanical Systems, World Scientific, 2003.
[3] R. Andrzejewski, J. Awrejcewicz, Nonlinear Dynamics of a Wheeled Vehicle, Springer, 2005.
[4] R.S. Sharp R S, D.A. Crolla, Road vehicle suspension system design – a review, Veh. Syst. Dyn. 16 (1987) 167–192.
[5] D. Cao, X. Song, Mahdi Ahmadian Editors' perspectives: road vehicle suspension design, Veh. Syst. Dyn. 49 (1-2) (2011).
[6] Z. Lozia, The use of a linear quarter-car model to optimize the damping in a passive automotive suspension system – a follow-on from many authors' works of the recent 40 years, Arch. Autom. Eng. – Archiwum Motoryzacji 71 (1) (2016) 39–71.
[7] V.M. Barethiye, G. Pohit, A. Mitra, Analysis of a quarter car suspension system based on nonlinear shock absorber damping models, Int. J. Autom. Mech. Eng. 4 (3) (2017) 4401–4418.
[8] B. Brogliatto, A.A.T. Dam, L. Paoli, F. Genot, M. Abadie, Numerical simulation of finite dimensional multibody nonsmooth mechanical systems, Appl. Mech. Rev. 55 (2) (2002) 107–150.
[9] C. Glocker, C. Studer, Formulation and preparation for numerical evaluation of linear complementarity systems in dynamics, Multibody Syst. Dyn. 13 (2005) 447–463.
[10] T. Fuisawa, E.S. Kuh, Piecewise-linear theory of nonlinear networks, SIAM J. Appl. Math. 22 (2) (1972) 307–328.
[11] L.O. Chua, S.M. Kang, Section-wise piecewise-linear functions: canonical representation, properties, and applications, Proc. IEEE 65 (6) (1977) 915–929.
[12] L.O. Chua, Chua's Circuit 10 years later, Int. J. Circuit Theory Appl. 22 (4) (1994) 279–305.
[13] C.H. Lamarque, O. Janin, J. Awrejcewicz, Chua systems with discontinuities, Int. J. Bifurcation Chaos 9 (4) (1999) 591–616.
[14] J. Awrejcewwicz, M.L. Calvisi, Mechanical models of Chua's circuit, Int. J. Bifurcation Chaos 12 (4) (2002) 671–686.
[15] W. Grzesikiewicz, Dynamics of mechanical systems with constraints, Prace Naukowe Politechniki Warszawskiej. Mechanika (117) (1990) Nrin Polish.
[16] F. Pfeiffer, C. Glocker, Multibody Dynamics with Unilateral Contacts, Willey&Sons, N.York, 1996.
[17] B. Armstrong-Helouvry, P. Dupont, C. Canudas de Wit, a survey of models, analysis tools and compensation methods for the control of machines with friction, Automatica 30 (7) (1994) 1083–1138.
[18] M. Nordin, P.O. Gutman, Controlling mechanical systems with backlash – a survey, Automatica 38 (2002) 1633–1649.
[19] E.D. Sontag, Nonlinear regulation: the piecewise linear approach, IEEE Trans. Autom. Control AC-26 (2) (1981) 346–358.

[20] V.M. Veliov, M.I. Krasnov, Controllability of piecewise linear systems, Syst. Control Lett. (5) (1986) 335–341.
[21] S.P. Banks, S.A. Khathur, Structure and control of piecewise-linear systems, Int. J. Control 50 (2) (1989) 667–686.
[22] A. Rantzer, M. Johanson, Piecewise linear quadratic optimal control, IEEE Trans. Autom. Control 45 (4) (2000) 629–637.
[23] T.A.M. Kevenaar, D.M.W. Leenaerts, A comparison of piecewise-linear model descriptions, IEEE Trans. Circuit Syst. 39 (12) (1992) 996–1004.
[24] E.C. Servetas, C.A. Karybakas, Synthesis of piecewise linear characteristics, Int. J. Control 8 (2) (1968) 101–112.
[25] G.A. Korn, Trick and treats: nonlinear operations in digital simulation, Math. Comput. Simul. 29 (1987) 129–143.
[26] D. Żardecki, The luz(...) and tar(...) projections – a theoretical background and an idea of application in a modeling of discrete mechanical systems with backlashes or frictions, Biuletyn WAT L (5) (2001) 125–160 Nrin Polish.
[27] D. Żardecki, Piecewise Linear luz(...) and tar(...) Projections. Part 1 – Theoretical Background, J. Theor. Appl. Mech. 44 (1) (2006) 163–184.
[28] D. Żardecki, Piecewise Linear luz(...) and tar(...) Projections. Part 2 – application in modeling of dynamic systems with freeplay and friction, J. Theor. Appl. Mech. 44 (1) (2006) 185–202.
[29] D. Żardecki, Modelling of freeplay and friction based on luz(…) and tar(…) projections – theory and application in simulation studies of nonlinear vibrations in car steering systems, Habilitation monograph, Ed. WAT, Warsaw (2007) in Polish.
[30] D. Żardecki, Structural sensitivity analysis of non-smooth systems, in: Proceedings of the 9th DSTA Conference, Łódź, 2007.
[31] D. Żardecki, Piecewise linear modeling of friction and stick-slip phenomenon in discrete dynamical systems, J. Theor. Appl. Mech. 44 (2) (2006) 255–277.
[32] D. Żardecki, Static friction indeterminacy problems and modeling of stick-slip phenomenon in discrete dynamic systems, J. Theor. Appl. Mech. 45 (2) (2007) 289–310.
[33] Z. Lozia, D. Żardecki, Vehicle dynamics simulation with inclusion of freeplay and dry friction in steering system (SAE Paper 2002-01-0619). SAE 2002 Transactions, J. Passenger Cars – Mech. Syst. (2002) 907–923.
[34] Z. Lozia, D. Żardecki, Dynamics of steering system with freeplay and dry friction – comparative simulation investigation for 2WS and 4WS Vehicles, in: Proceedings of the Steering and Suspension, Tires and Wheels Symposium World Congress, Detroit, 2005, pp. 1–10.
[35] D. Żardecki, A. Dębowski, Examination of computational procedures from the point of view of their applications in the simulation of torsional vibration in the motorcycle steering system, with freeplay and friction being taken into account, The Arch. Autom. Eng. 64 (2) (2014) 179–195.
[36] D. Żardecki, A. Dębowski, Method of analyzing torsional vibrations in the motorcycle steering system in the phase plane, The Arch. Autom. Eng. 76 (2) (2017) 137–154.
[37] D. Żardecki, Non-smooth model of suspension based on piecewise-linear luz(…) and tar(…) projections, in: Proceedings of the 15th DSTA Conference, Łódź, 2019.